Parietofrontal network upregulation after motor stroke

M. Bönstrup[a,b,*], R. Schulz[a], G. Schön[c], B. Cheng[a], J. Feldheim[a], G. Thomalla[a], C. Gerloff[a]

[a] Department of Neurology, University Medical Center Hamburg-Eppendorf, Germany
[b] Human Cortical Physiology and Neurorehabilitation Section, National Institute of Neurological Disorders and Stroke, National Institutes of Health, Bethesda, MD, USA
[c] Department of Medical Biometry and Epidemiology, University Medical Center Hamburg-Eppendorf, Germany

ABSTRACT

Objective: Motor recovery after stroke shows a high inter-subject variability. The brain's potential to form new connections determines individual levels of recovery of motor function. Most of our daily activities require visuomotor integration, which engages parietal areas. Compared to the frontal motor system, less is known about the parietal motor system's reconfiguration related to stroke recovery. Here, we tested if functional connectivity among parietal and frontal motor areas undergoes plastic changes after stroke and assessed the behavioral relevance for motor function after stroke.
Methods: We investigated stroke lesion-induced changes in functional connectivity by measuring high-density electroencephalography (EEG) and assessing task-related changes in coherence during a visually guided grip task with the paretic hand in 30 chronic stroke patients with variable motor deficits and 19 healthy control subjects. Quantitative changes in task-related coherence in sensorimotor rhythms were compared to the residual motor deficit.
Results: Parietofrontal coupling was significantly stronger in patients compared to controls. Whereas motor network coupling generally increased during the task in both groups, the task-related coherence between the parietal and primary motor cortex in the stroke lesioned hemisphere showed increased connectivity across a broad range of sensorimotor rhythms. Particularly the parietofrontal task-induced coupling pattern was significantly and positively related to residual impairment in the Nine-Hole Peg Test performance and grip force.
Interpretation: These results demonstrate that parietofrontal motor system integration during visually guided movements is stronger in the stroke-lesioned brain. The correlation with the residual motor deficit could either indicate an unspecific marker of motor network damage or it might indicate that upregulated parietofrontal connectivity has some impact on post-stroke motor function.

1. Introduction

The basis of spontaneous recovery from a motor stroke in humans is unclear. Given a window of heightened microstructural plasticity (Rossini et al., 2003; Ward, 2017) and evidence for dynamic reconfiguration of cortical areas engaged in motor activity after stroke (Grefkes and Fink, 2011), it is conceivable that interaction patterns between cortical areas reorganize after a lesion. Unravelling common patterns of neuroplastic processes that lead to regain of motor function is a major challenge of neurorehabilitative medicine and a prerequisite for a mechanistic approach of interventional therapies.

During physiologic motor activity, the primary and secondary motor areas engage in balanced facilitatory and inhibitory interactions (Bonstrup et al., 2016; Grefkes et al., 2008a). After a motor stroke, in the acute phase, the facilitatory coupling among the frontal motor areas, i.e. ventral premotor cortex (PMv), the supplementary motor area (SMA) and the primary motor cortex (M1) in the contralateral (ipsilesional) hemisphere appears to be disrupted; and to normalize along with recovery (Rehme et al., 2011b). Most of our daily activities require precise interaction between visual perception and the motor system. For higher order movements, that require visuomotor and sensorimotor integration (Vingerhoets, 2014) as well as for reaching and grasping (Bernier et al., 2017; Corbetta and Shulman, 2002; Grefkes et al., 2004; Konen et al., 2013), parietal motor areas are

specifically engaged. However, their relative role in motor system reconfiguration after stroke is less well understood compared to the frontal brain. Conceivably, parietofrontal pathways are of high importance for post-stroke rehabilitation (Wu et al., 2014). Recently, it was shown that lesion-induced network plasticity involves parietofrontal motor pathways connecting PMv with the anterior intraparietal sulcus (aIPS) (Schulz et al., 2015). And in functional magnetic resonance imaging (fMRI), it was demonstrated that reciprocal facilitatory connectivity between the aIPS and M1 in the ipsilesional hemisphere is enhanced in well-recovered chronic stroke survivors compared with healthy participants during a visually guided grip task (Schulz et al., 2016). However, the functional relevance of parietofrontal network upregulation for motor function has not been characterized yet. Whether the abnormally increased parietofrontal connectivity in stroke survivors is systematically varying with the degree of paresis, is a highly intriguing question not only for deeper pathophysiologic understanding, but also to substantiate the validity and importance of this connection as a tentative target for non-invasive brain stimulation protocols.

We recorded high-density EEG during a visually guided grip task with the paretic hand in 30 chronic stroke patients (we use the term chronic in agreement with previous definitions and use (Di Pino et al., 2014; Ward et al., 2003)) and 19 healthy control subjects.

We first set out to reproduce the previous finding of enhanced facilitatory coupling between the parietal and motor cortex in a larger patient cohort and with a different method to detect brain connectivity: Across perceptual, cognitive and motor systems, synchronization of oscillations has been detected as a key mechanism of how transient coalitions of neural populations at small- and large spatial scales commit to a common task (communication through coherence concept) (Bonnefond et al., 2017; Siegel et al., 2012). We hypothesized that parietal and frontal motor areas would show higher coherence during the task for patients than for control participants. Secondly, we hypothesized that higher coherence parameters are found in patients with a stronger residual motor deficit.

2. Participants and methods

2.1. Participants

30 patients (19 male, 1 left-handed, aged 65 ± 13 years, mean ± std) were included three months (104 ± 17 days) after first-ever ischemic stroke causing a motor deficit involving hand function (five subcortical, 25 cortical/cortico-subcortical). 14 patients had lesions to the dominant hemisphere. Initial and residual motor impairment was determined by means of grip force, the Nine-Hole Peg Test performance (NHP), and the Fugl–Meyer score for the upper extremity (UEFM) 3–5 days after stroke and 3 months after stroke. For the grip force and the NHP, behavioral scores were calculated as proportional values (affected/unaffected hand), whereas in case of the NHP, prior to normalization the score for each hand was expressed as pegs/s to give a performance value. Individual motor recovery values were obtained by calculating the difference between initial and residual behavioral scores. A group similar in age and gender ($n = 19$, 10 males, one left-handed, aged 64.8 ± 11.1 years) served as controls. The study design was approved by the local ethical committee. All participants gave their written informed consent according to the ethical declaration of Helsinki.

2.2. Motor task

Participants underwent EEG during a simple motor task which required them to perform isometric visually guided whole hand grips with the paretic hand using a grip-force device (Grip Force Bimanual, Current Designs, Inc., Philadelphia, USA). The control participants were randomly assigned to use the left or right hand in a distribution

matching the lesion-side of the patient group (nine right hand). Participants were seated comfortably in an armchair with the right and left arm relaxed positioned in their lap, each holding one of the bimanual grip-force devices. We compared two conditions of varying target grip force, one keeping the force constant across the group (constant output of 5 kg) and the other keeping the task effort constant across the group (constant effort of 20% MVC). Each condition was recorded with 20 repetitions of a 9 s constant grip hold phase. The begin of each grip as well as continuous feedback about the applied force were provided visually by the appearance and vertical level of a horizontal bar on a screen. The participants were instructed to lift the bar into the target zone (paralleling the target force of either 5 kg (= constant-output) or 20% of maximal force (= constant-effort)) and hold it constant until it disappeared (after 9 s, Supplementary Fig. 1). Participants were instructed to avoid eye movements and fixate the bar, whose level was within a small visual angle of ± 5°, thus not requiring large amplitude eye movements during the force build-up. During the inter-trial interval of 12 ± 2 s, participants were instructed to fixate a cross in the center of the screen and relax. To assess bilateral movements, the force applied with the (unaffected) non-active hand was continuously monitored throughout the hand grip as the patient held a grip force device in both hands. If necessary, breaks were introduced depending on the participant's needs. The task was described in the previous report on functional MRI (fMRI) derived effective coupling (Schulz et al., 2016) and in (Bonstrup et al., 2015).

2.3. Data acquisition

2.3.1. Electroencephalography

The EEG was recorded from 63 cephalic active surface electrodes, referenced to a nose-tip or Cz-electrode during recording (interim replacement of recording setup). One electrode was mounted below the left eye for electrooculogram recording. Before and after each experimental session, a resting state was recorded for 3–4 min with eyes fixed on a cross in the center of the screen. See Supplementary material section 1.1 for details on the recording setup.

2.4. Data analysis

2.4.1. EEG data preprocessing

The continuous EEG was offline down sampled to 125 Hz, detrended and subjected to an independent component analysis (logistic infomax ICA; (Makeig et al., 1996)) to remove eye-blink artifacts. The 20 trials of each grip condition were segmented in epochs of 1 s duration covering the hold phase, starting 1 s after the beginning of each trial until the end (20 × 8 s). The resting state condition was likewise segmented into epochs of 1 s. Trials were then visually inspected to reject remaining artifacts (number of 1 s long trials after artifact rejection (mean ± std): task 119 ± 14, rest 235 ± 29). See Supplementary material section 1.2 for details on the preprocessing.

2.4.2. Source reconstruction and spectral power and coherence analysis

We reconstructed source space activity and connectivity in the parietofrontal motor network using spatial filtering. The network consisted of five ipsilesional regions of interest (ROIs) contralateral to the (affected) active hand, consisting of M1, PMv, SMA, and the aIPS and caudal part of the intraparietal sulcus (cIPS). Coordinates were predefined as reported previously ((Schulz et al., 2016), Suppl. Table 2). For each location, a linear constrained minimum variance (LCMV) beamforming filter was computed based on an individual forward model and a covariance matrix of sensor space time series. The choice of a beamforming approach for spatial filtering was based on previous publications in the field of motor stroke research using EEG or magnetoencephalography (MEG). Cross-spectra between each pair of sensors were calculated at frequency bands of interest using the continuous wavelet transformation with a width of 5 cycles. The cross-spectra were

then projected to source space using the spatial filter to derive source spectral power and coherence. See Supplementary material section 1.3 for details. We focused spectral analyses on three frequency bands (low alpha 8–10 Hz, high alpha 11–13 Hz, beta 18–22 Hz) that are known to be consistently modulated by motor activation (Crone et al., 1998; Salenius et al., 1997) and show distinct patterns of task-related amplitude (Rossiter et al., 2014) and coupling changes in chronic stroke patients (Gerloff, 2006).

2.4.3. Task-related spectral power and coherence analysis

For normalization of the underlying distribution, spectral power estimates were log-transformed and coherence estimates were subjected to a hyperbolic inverse tangent ($\tanh^{-1}$) transformation. As a second step, to reduce inter-subject variability, the source spectral power and coherence estimates recorded during task execution were normalized with the spectral estimates during rest (Gerloff et al., 2006). Together, task-related spectral power (TR-Pow) and task-related coherence (TR-Coh) were derived using the following formula:

$$\text{TR-Pow} = \log(\text{Pow}_{\text{activation}}) - \log(\text{Pow}_{\text{rest}})$$

$$\text{TR-Coh} = \tanh^{-1}(\text{Coh}_{\text{activation}}) - \tanh^{-1}(\text{Coh}_{\text{rest}})$$

2.5. Statistics

The statistical analyses were done with R Version 3.2.5 (R Team, 2015) and MATLAB Version 2011a. To assess differences in TR-Pow and TR-Coh in the parietofrontal motor network between chronic stroke patients and the control group, we iteratively ran a linear mixed effects (LME) model (Bonstrup et al., 2015) using the lmer function provided in the lmerTest package (Kuznetsova et al., 2015) for TR-Pow at each region (five ROIS) or TR-Coh between all pairs of regions (10 connections) at each of the predefined frequency bands within the parietofrontal motor network (15 and 30 models, respectively). The models were designed to explain variance in TR-Pow and TR-Coh with the fixed effect GROUP (two level factor: patient and control), grip TASK (two level factor: constant grip force of 5 kg or 20% of MVC) and subject ID as a random intercept. Each factors' predictive power was assessed using analysis of variance and if insignificant, the factor was dropped. The same statistical framework was used to assess the relationship between TR-Coh and motor function in each group individually, by explaining variance in TR-Coh with the fixed effect relative (affected/ unaffected side) grip force (GRIP), NHP or UEFM score, alone and in interaction with the individual motor recovery values. Each model's validity was assessed via diagnostic plots of the model's residuals to assess normal distribution and homoscedasticity. The whole brain source spectral power maps in Supplementary Fig. 3 were thresholded using one-sample t-tests at each frequency and source location ($p < 0.05$, corrected for multiple comparisons using False discovery rate (FDR) correction according to Benjamini and Hochberg for 8214 tests at an alpha-level of 0.05 (Benjamini and Hochberg, 1995)).

3. Results

3.1. Clinical data

The patient group ($n = 30$) mostly consisted of well-recovered (UEFM > 60, $n = 24$) chronic stroke patients (Di Pino et al., 2014; Rehme et al., 2012), with a few moderate (UEFMA > 40, $n = 3$) to poorly-recovered (UEFMA $\leq$ 40, $n = 3$) patients. Of the well-recovered patients, five initially had a severe motor impairment (UEFMA $\leq$ 40), while another five had a moderate motor impairment (UEFMA > 40 & $\leq$60). The clinical data are given in Table 1, and a stroke lesion map is plotted in Fig. 1. Four out of the 30 patients were unable to fully reach the target force of 5 kg due to residual paresis and one patient was unable to generate any force at all. In these cases, patients were

instructed to build up as much force as possible to lift the bar. During the motor task, four of the patients showed co-contraction of the unaffected hand in the constant-output task, and two patients in the constant-effort task, at a level within the detection sensitivity of the grip device (0.026–10 kg). Supplementary Fig. 2 depicts the time course of exerted grip force in the active and contralateral hand during each condition for each patient.

3.2. Task-related spectral power

In a whole brain spectral power analysis, there were significant TR-Pow decreases in the lower and upper alpha as well as beta bands over bilateral primary somatosensory cortices, premotor cortices and SMA. Supplementary Fig. 3 depicts whole brain group averaged spectral power maps rendered on the cortical surface for each group and frequency range. In the alpha frequency range, the TR-Pow decrease also involved the parietal cortices, as in the blood-oxygen-level dependent (BOLD)-activation maps reported in our previous study (Schulz et al., 2016). At the ROI within the parietofrontal motor network, both groups showed significant TR-Pow decreases at parietal and frontal motor areas. Regarding differences in TR-Pow reductions between patients and control group, there were no significant regions in the whole-brain topographical maps (two-sample t-test $p < 0.05$, FDR-corrected for 8214 comparisons). Looking specifically at the parietofrontal ROI, a statistical group difference in the beta band was only found at the aIPS and cIPS (LME, factor GROUP $p = 0.03$ at both ROI), whereas in both alpha bands, no statistical differences were found (Supplementary Table 1). Of note, this absence of systematic differences in spectral power between the two groups renders it unlikely that the observed differences in connectivity (see below) resulted from different signal-to-noise ratios between groups (Siegel et al., 2012). We found no significant difference between the TR-Pow decreases in both force levels (constant output of 5 kg and constant effort of 20% MVC across the group, factor TASK, (Supplementary Table 2)). This reproduces a previous finding in a smaller but overlapping patient group (Bonstrup et al., 2015).

3.3. Parietofrontal functional connectivity

In general, functional coupling within the parietofrontal motor network increased during the grip task. Both groups showed significant parietofrontal coupling predominantly in the alpha bands (aIPS-M1, cIPS-M1, cIPS-PMv, aIPS/cIPS-SMA) as well as frontomesiocentral coupling in the alpha bands (PMv-SMA). In both groups, less coupling was evident in the beta band. The most consistent finding over all frequency bands and strongest numerical difference in coupling between stroke patients and control participants was the connection between aIPS and M1. In stroke patients, we detected an increase in coupling between the aIPS and M1 which was significantly larger than in the control group and generalized over frequency bands (lower alpha: TR-Coh difference Stroke-Controls 0.2, $p = 0.003$, upper alpha: 0.2, $p = 0.008$, beta: 0.19, $p = 0.010$, LME factor GROUP). Since coherence quantifies synchronization based on phase and amplitude and we detected large spectral power reductions in both groups, we confirmed the result by computing the phase locking value as a synchronization measure (see Supplementary material 1.3). We likewise found that the coupling between aIPS and M1 was exclusively (within the parietofrontal network) and consistently (over all frequency bands) increased and stronger in the patient group (Supplementary Table 5). Fig. 2 topographically illustrates significant coupling changes of the network for each group and the statistical comparison between groups for the lower alpha band (8–10 Hz, see Supplementary material Fig. 4 for topographical plots of coupling in the upper alpha and beta rhythm). Although obtained with a completely different method and based on a very different concept of neuronal coupling, these findings replicate previously reported coupling estimates derived from a DCM

Table 1
Clinical data.

ID	Sex	Age	Handedness	Stroke	Stroke location	Initial NIHSS	Initial grip force	Initial NHP	Initial UEFM	TAS (days)	Residual grip force	Residual NHP	Residual UEFM
1	M	62	Right	Left	CI, CR	3	0.2	0.2	37	95	0.7	1.0	62
2	F	49	Right	Left	CI, CR, BG, INS	10	0	0	4	168	0.12	0	13
3	M	68	Left	Right	CI, CR, BG, INS	3	0.5	0	62	117	0.8	0.5	62
4	F	68	Right	Right	PON	5	0.6	0.55	61	102	0.9	0.8	62
5	M	70	Right	Right	CR	1	0.42	0.41	62	90	0.71	0.78	65
6	M	65	Right	Left	CI, CR, INS	3	0.9	0.8	65	104	1.0	1.1	66
7	F	73	Right	Right	CI, CR, BG	3	0.8	0.7	62	124	0.8	0.7	65
8	M	58	Right	Right	PON	7	0	0	7	146	0.6	0.8	58
9	M	53	Right	Left	MED	4	0.53	0.81	62	89	0.8	0.95	66
10	M	73	Right	Left	CI, CR	9	0	0	4	116	0	0	13
11	M	50	Right	Right	CI, BG, INS, MFG	7	0	0	20	85	0.72	0.63	60
12	M	70	Right	Right	CR	0	0.8	0.8	65	100	1.0	0.9	66
13	M	53	Right	Right	CI, BG	4	0.80	0.7	65	92	0.88	0.85	66
14	F	81	Right	Right	CR	1	0.9	0.7	65	90	1.5	0.7	66
15	F	78	Right	Left	CR	5	0.8	0.8	65	99	0.7	1.0	64
16	F	55	Right	Right	PRC	1	0.8	0.6	63	96	0.9	0.8	65
17	M	48	Right	Left	CR, SPL, MFG	3	0.53	0.24	56	97	1.06	1.06	66
18	M	63	Right	Left	CR	3	0.3	0.2	42	101	0.7	1.0	63
19	F	70	Right	Right	CR, BG, INS	5	0.4	0.2	56	96	0.7	0.6	58
20	F	85	Right	Right	CR, INS	7	0	0	5	90	0.35	0	40
21	M	81	Right	Left	PONS	4	0.53	0	25	90	1.08	1	64
22	M	44	Right	LEFT	CR, PRC, MFG, SFG, POC, LOC, MTG, ITG, STG	8	0.84	0.33	61	103	0.97	0.75	66
23	F	78	Right	LEFT	CI, BG	0	1.1	1.2	66	116	1.2	1.1	66
24	F	47	Right	Right	BG, CI, FP, CR, PRC, SPL, POC, PREC, SFG, LOG	2	0.11	0	32	93	0.69	0.56	66
25	M	53	Right	Left	BG, CI	5	0.68	0.41	41	93	1.19	1	64
26	M	80	Right	Left	CR	4	0.62	0	57	106	0.82	0.69	65
27	M	76	Right	Left	PONS	5	0.15	0	26	108	1.14	0.96	66
28	M	55	Right	Left	BG, CI, CR	0	0.9	1	66	100	1.14	1.11	66
29	M	48	Right	Left	BG, CI CR, STG, INS	7	0.78	0	43	94	1.14	0.8	65
30	F	87	Right	Left	CR	1	0	0	32	117	0.87	0.91	64
Mean ± std	19 M, 11 F	65 ± 13	29 R, 1 L	13 R, 17 L		4 ± 3	0.5 ± 0.34	0.36 ± 0.36	46 ± 21	104 ± 17	0.84 ± 0.3	0.77 ± 0.3	60 ± 13.5

Age is given in years. Grip force and NHP values are given in proportional values (affected/unaffected hand). Initial NIHSS, grip force and NHP taken 3–5 days post stroke. Residual NIHSS, grip force and NHP after passage of TAS, time after stroke in days. BG indicates basal ganglia; CI, internal capsule; CR, corona radiata; F, female; FP, frontal pole; INS, insula; ITG, inferior temporal gyrus; LOC, lateral occipital cortex; L, left; M, male; medulla oblongata, MED; middle frontal gyrus, MFG; middle temporal gyrus, MTG; NHP, Nine-Hole Peg Test performance; NIHSS, National Institute of Health Stroke Scale; PON, pons; postcentral gyrus, POC; PRC, precentral gyrus; precuneus, PRE; R, right; superior frontal gyrus, SFG; superior parietal lobule, SPL; superior temporal gyrus, STG; and UEFM, upper extremity Fugl–Meyer score.
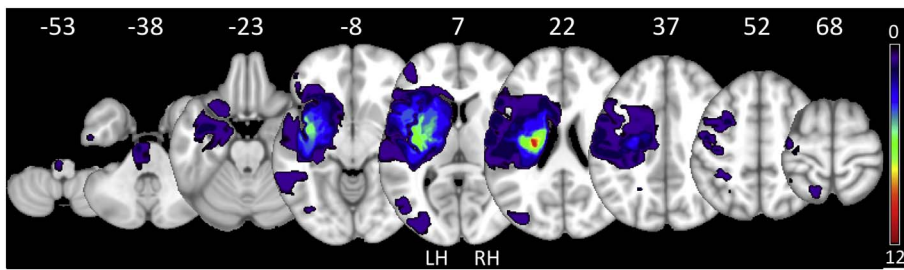
Fig. 1. Lesion overlay. Summary overview of lesion locations in all 30 stroke patients with color indicating frequency of lesions. Right-sided lesions were mirrored to the left (LH-left hemisphere; RH-right hemisphere). All lesions are registered to normal space and displayed on a T1 template in Montreal Neurological Institutes (MNI) standard space, z-values of representative slices are given. Images were obtained using a high-resolution 3D magnetization-prepared, rapid acquisition gradient-echo sequence (MPRAGE). (For interpretation of the references to color in this figure legend, the reader is referred to the web version of this article.)

study based on fMRI data collected in an overlapping but smaller study population implementing the same grip task (Schulz et al., 2016). Excluding patients that performed the task but were unable to reach the target grip force did not change the resulting coupling patterns. The task effort (constant grip force of 5 kg or 20% of MVC) had no additional explanatory value for the TR-Coh of any connection within the network (Supplementary Table 3). For a comprehensive tabulation of mean coupling estimates for all frequency bands, see Table 2.

3.4. Prediction of parietofrontal connectivity by residual motor deficit

If the functional connectivity between aIPS and M1 of the ipsilesional hemisphere is enhanced in stroke patients compared with controls, we postulated that the strength of this connection should be inversely related to individual motor impairment. To test this, we used the relative (affected/unaffected side) grip force, NHP as well as the UEFM score to explain variance in parietofrontal connectivity in the stroke patient group. Each of these measures reflects different motor skills and visuomotor integration demands: The NHP relies on fine motor skills and dexterity, the grip force reflects muscle strength and the UEFM indicates active movement range and synergies of proximal and distal muscles. We found that the strength of TR-Coh between the aIPS and M1 in the alpha bands of the lesioned hemisphere could be predicted by the variance in residual fine motor skills as measured by NHP (LME, factor NHP lower alpha: $p = 0.022$, upper alpha: $p = 0.044$) and in the grip force in the upper alpha and beta bands (LME, factor GRIP upper alpha: $p = 0.045$, beta: $p = 0.007$, Table 3). An increase in 10% of grip force was related to a decrease in TR-Coh of 0.025 (lower alpha), 0.033 (upper alpha) or 0.043 (beta). Additionally, an increase in 10% of NHP was related to a decrease in TR-Coh of 0.031 (lower alpha) and 0.033 (upper alpha) as seen in Fig. 3. Including the task effort (constant grip force of 5 kg or 20% of MVC) into the statistical model of grip force and TR-Coh in the upper alpha and beta bands led to no significant model improvement (LME, interaction GRIP x TASK upper alpha: $p = 0.47$, beta: $p = 0.84$). In the control group, we found no significant relationship between grip force and TR-Coh between aIPS and M1 (Supplementary Table 4).
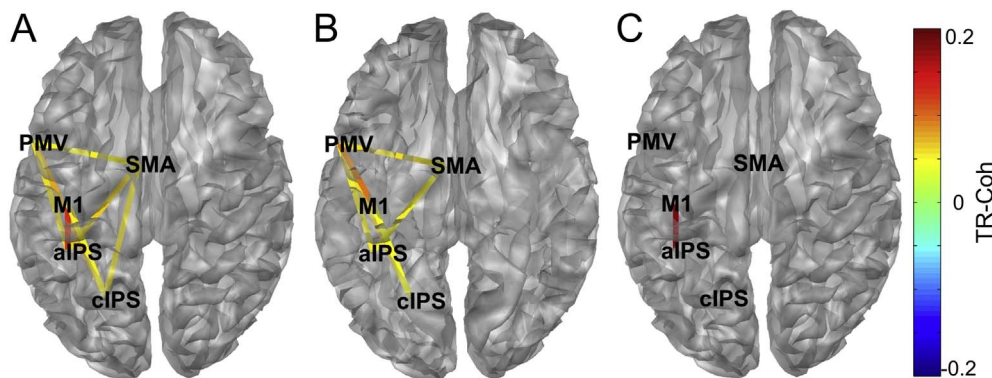
Patients with a high grip force or NHP three months post stroke are either mildly affected by the infarction (high initial motor function, Table 1) or well recovered (low initial motor function, Table 1). To learn about the role of the detected relationship between parietofrontal connectivity and the residual motor deficit for motor recovery, we tested whether motor recovery (quantified by the improvement in motor function from the initial assessment 3–5 days post stroke to the late assessment three months after stroke), would show a significant interaction with the motor performance values in explaining TR-Coh (Fig. 3). Such an interaction would be reflected in a different slope in the relationship between TR-Coh and residual motor function for patients with a high and low motor recovery. However, including motor recovery in the model for any of the frequency bands or motor performance tests did not explain additional variance, indicating that well recovered and mildly affected patients show low parietofrontal connectivity, as the control participants.

4. Discussion

We investigated connectivity between parietal and frontal motor areas during a grip task in 30 chronic stroke patients and 19 healthy control subjects and found a significantly stronger interaction between the aIPS and M1 in the stroke patients. Although parietofrontal coupling generally increased during the task in both groups, only the connection between the aIPS and M1 proved to be significantly enhanced in the ipsilesional hemisphere in patients, that is, contralateral to the affected upper extremity; this pattern generalized across the alpha and beta rhythms. Having utilized a completely different imaging modality, this finding successfully replicates results of previous investigations in which parietofrontal motor connectivity was assessed using fMRI and DCM, thereby substantiating the physiologic importance and validity of this connection independent of neuroimaging modality or choice of data analysis tools (Schulz et al., 2016). Furthermore, and importantly, in this larger patient group we found that the increased task-induced coupling was significantly related to residual motor deficit. A possible interpretation is that this intensified cross-talk between parietal and frontal motor areas subserves for post-

Fig. 2. Topography of significant TR-Coh changes in the lower alpha band (8–10 Hz). A) chronic stroke patients B) control group (one-sample t-test of TR-Coh against 0, $p < 0.05$) and C) the difference between the two groups ([Patients-Controls]; LME, fixed effect GROUP, $p < 0.05$). Warm colors indicate TR-Coh increases during the grip task compared to resting state ('enhanced synchrony') and cold colors indicate decreases. aIPS indicates anterior part of the intraparietal sulcus; cIPS, caudal part of the intraparietal sulcus; M1, primary motor cortex; PMv, ventral premotor cortex; and SMA, supplementary motor area. Hemispheres were mirrored for statistical and display purposes in cases where the contralateral active hemisphere was the right. Topographic plots for the upper alpha and beta band can be found in the Supplementary material (Supplementary Fig. 4). (For interpretation of the references to color in this figure legend, the reader is referred to the web version of this article.)

Table 2
Mean TR-Coh changes during the hand grip relative to rest with corresponding 95% confidence interval for stroke patients and control participants (A), as well as the group difference (TR-Coh stroke–controls) and corresponding p-values (LME fixed effect GROUP).

A

	Stroke									Control								
	Lower alpha			Upper alpha			Beta			Lower alpha			Upper alpha			Beta		
	Mean	95% conf.		Mean	95% conf.		Mean	95% conf.		Mean	95% conf.		Mean	95% conf.		Mean	95% conf.	
		Low.	Upp.		Low.	Upp.		Low.	Upp.		Low.	Upp.		Low.	Upp.		Low.	Upp.
cIPS-aIPS	0.00	−0.04	0.04	0.00	−0.04	0.04	−0.04	−0.06	−0.02	0.02	−0.05	0.08	0.02	−0.05	0.10	−0.01	−0.05	0.03
aIPS-M1	0.13***	−0.07	0.30	0.10*	−0.08	0.30	0.12*	−0.08	0.30	−0.07	−0.07	−0.06	−0.1**	−0.07	−0.10	−0.06	−0.08	−0.05
cIPS-M1	0.05**	−0.03	0.10	0.04*	−0.04	0.10	0.03	−0.03	0.08	0.05*	−0.04	0.10	0.05**	−0.04	0.10	0.02	−0.04	0.08
aIPS-PMV	0.06***	−0.03	0.10	0.00	−0.03	0.04	−0.03	−0.04	−0.01	0.06*	−0.05	0.20	0.00	−0.05	0.05	0.00	−0.04	0.04
cIPS-PMV	0.08***	−0.03	0.20	0.07***	−0.03	0.20	0.02	−0.02	0.06	0.06***	−0.03	0.20	0.04**	−0.03	0.10	0.01	−0.02	0.04
M1-PMV	0.02	−0.04	0.09	0.02	−0.03	0.06	0.00	−0.03	0.03	0.1*	−0.09	0.30	0.09*	−0.08	0.30	0.05	−0.08	0.20
aIPS-SMA	0.06***	−0.03	0.20	0.05**	−0.03	0.10	0.03	−0.03	0.09	0.05*	−0.05	0.20	0.02	−0.03	0.06	−0.02	−0.04	0.00
cIPS-SMA	0.06***	−0.02	0.10	0.08***	−0.02	0.20	0.04*	−0.03	0.10	0.02	−0.03	0.08	0.04*	−0.03	0.10	0.00	−0.03	0.03
M1-SMA	0.03	−0.04	0.09	0.00	−0.03	0.04	0.02	−0.04	0.08	−0.01	−0.08	0.06	−0.02	−0.08	0.04	−0.04	−0.08	0.00
PMV-SMA	0.06***	−0.03	0.10	0.01	−0.02	0.05	−0.01	−0.03	0.01	0.06*	−0.06	0.20	0.04	−0.05	0.10	−0.02	−0.05	0.01

Stars indicate significant changes within the group (one-sample t-test, $*p < 0.05$, $**p < 0.01$, $***p < 0.001$)

B

	Lower alpha		Upper alpha		Beta	
	Diff.	p-Value	Diff.	p-Value	Diff.	p-Value
cIPS_aIPS	−0.02	0.60	−0.02	0.50	−0.03	0.60
aIPS_M1	0.2**	0.00	0.2**	0.01	0.19**	0.01
cIPS_M1	0.01	0.70	−0.02	0.60	0.01	0.90
aIPS_PMV	0.00	1.00	0.00	1.00	−0.02	0.40
cIPS_PMV	0.02	0.50	0.03	0.30	0.01	0.70
M1_PMV	−0.08	0.10	−0.07	0.10	−0.05	0.20
aIPS_SMA	0.01	0.80	0.03	0.20	0.05	0.06
cIPS_SMA	0.04	0.09	0.04	0.05	0.04	0.10
M1_SMA	0.04	0.30	0.02	0.60	0.06	0.20
PMV_SMA	0.00	0.90	−0.03	0.40	0.01	0.50

Stars indicate significant changes across the group (LME, factor GROUP, $**p < 0.01$).

Table 3

Regression coefficients with 95% Confidence Interval of fixed effect clinical score (grip force, NHP, UEFM) for coupling strength at each ROI and frequency band in stroke patients. Grip force and NHP performance were both modeled as proportional values (affected/unaffected hand).

	Lower alpha			Upper alpha			Beta		
	95% conf.			95% conf.			95% conf.		
	Coef.	Lower	Upper	Coef.	Lower	Upper	Coef.	Lower	Upper
GRIP									
cIPS aIPS	0.00	−0.19	0.18	−0.05	−0.20	0.14	−0.23	−0.50	0.02
aIPS M1	−0.25	−0.52	0.02	−0.33*	−0.60	−0.01	−0.43**	−0.70	−0.12
cIPS M1	0.01	−0.12	0.13	0.01	−0.10	0.15	−0.04	−0.20	0.07
aIPS PMV	0.00	−0.13	0.12	−0.03	−0.10	0.09	0.08	−0.08	0.24
cIPS PMV	−0.02	−0.13	0.10	−0.09	−0.20	0.03	−0.10*	−0.20	−0.02
M1 PMV	−0.02	−0.15	0.11	0.01	−0.10	0.13	0.04	−0.09	0.18
aIPS SMA	0.01	−0.11	0.13	−0.06	−0.20	0.05	0.06	−0.08	0.19
cIPS SMA	0.01	−0.08	0.10	0.02	−0.07	0.11	−0.02	−0.10	0.11
M1 SMA	−0.06	−0.21	0.08	−0.09	−0.20	0.05	0.02	−0.10	0.17
PMV SMA	−0.03	−0.13	0.08	0.01	−0.08	0.11	0.01	−0.09	0.12
Nine Hole Peg									
cIPS aIPS	−0.01	−0.19	0.17	−0.02	−0.21	0.16	−0.15	−0.40	0.10
aIPS M1	−0.31*	−0.57	−0.05	−0.33*	−0.65	−0.01	−0.20	−0.52	0.14
cIPS M1	−0.05	−0.18	0.07	−0.07	−0.21	0.07	−0.05	−0.16	0.07
aIPS PMV	−0.01	−0.14	0.11	−0.08	−0.20	0.03	0.13	−0.02	0.28
cIPS PMV	−0.04	−0.15	0.08	−0.09	−0.21	0.02	−0.02	−0.11	0.06
M1 PMV	−0.03	−0.15	0.10	−0.01	−0.13	0.11	0.04	−0.10	0.17
aIPS SMA	−0.01	−0.14	0.11	−0.02	−0.14	0.10	0.04	−0.09	0.17
cIPS SMA	0.03	−0.06	0.12	0.03	−0.06	0.13	0.01	−0.11	0.14
M1 SMA	−0.08	−0.22	0.07	−0.02	−0.16	0.12	0.10	−0.05	0.25
PMV SMA	−0.01	−0.11	0.11	0.01	−0.08	0.11	0.03	−0.07	0.14
UEFM									
cIPS aIPS	0.00	0.00	0.01	0.00	0.00	0.01	0.00	−0.01	0.01
aIPS M1	0.00	−0.01	0.00	0.00	−0.01	0.00	−0.01	−0.01	0.00
cIPS M1	0.00	0.00	0.00	0.00	0.00	0.00	0.00	0.00	0.00
aIPS PMV	0.00	0.00	0.00	0.00	0.00	0.00	0.004*	0.00	0.01
cIPS PMV	0.00	0.00	0.00	0.00	0.00	0.00	0.00	0.00	0.00
M1 PMV	0.00	0.00	0.00	0.00	0.00	0.00	0.00	0.00	0.00
aIPS SMA	0.00	0.00	0.00	0.00	0.00	0.00	0.00	0.00	0.00
cIPS SMA	0.00	0.00	0.00	0.00	0.00	0.00	0.00	0.00	0.00
M1 SMA	0.00	−0.01	0.00	0.00	0.00	0.00	0.00	0.00	0.01
PMV SMA	0.00	0.00	0.00	0.00	0.00	0.00	0.00	0.00	0.00

Stars indicate significant fixed effect of motor value (GRIP, NHP or UEFM) on TR-Coh (LME, *$p < 0.05$, **$p < 0.01$, uncorrected).

stroke motor function.

4.1. Relevance to neurorehabilitation research

This finding is of relevance for motor rehabilitation research for several reasons: First, the target identification process for brain stimulation protocols used in a neurorehabilitative setting requires robust pathophysiologic findings that become apparent independent of the specific methodology used in data acquisition and analysis. For detected 'abnormal' states in the stroke lesioned brain to be successfully translated from an exploratory study to a clinical interventional trial, a functionally relevant role of that state for therapeutic goals is mandatory. Second, the EEG provides direct information about neural activity as it reflects an aggregate measure of synaptic potential of cortical

neurons. There is recent converging evidence from animal and human invasive recordings that low-frequency oscillations in the electric field of the motor area (alpha and low-beta range) are directly linked to pyramidal neuron spiking activity (Haegens et al., 2011; Miller et al., 2012). Within the oscillatory code, information processing capacities of the brain are multiplexed through nested oscillations, and communication between neural populations is facilitated. Fries suggested a mechanism for neuronal communication through coherence (Fries, 2005). In this framework, coherence among neuronal groups ensures that they can interact effectively via the opening and closing of communication windows for input and output at the same time. The behavioral relevance for a synchronization of the low-frequency temporal reference frame among interacting regions has been abundantly reported across species, regions and cognitive systems (Arce-McShane
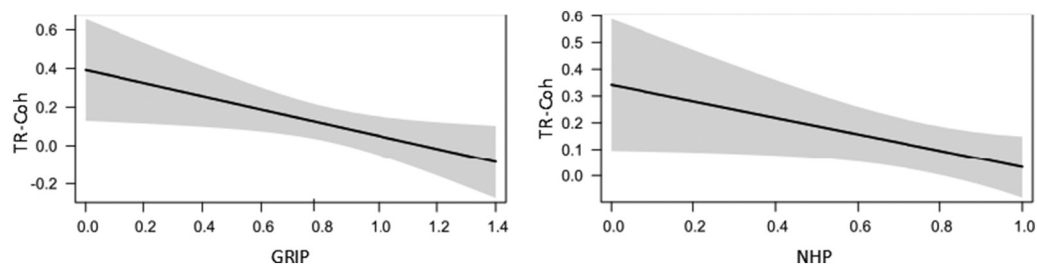

Fig. 3. Prediction of TR-Coh by motor deficit. Estimated TR-Coh values and 95% confidence intervals of the fixed effect residual motor deficit (separate models for GRIP and NHP) for the connection aIPS-M1 at the upper-alpha rhythm. Grip force and NHP were both modeled as proportional values (affected/unaffected hand).

et al., 2016; Gross et al., 2001; Hummel and Gerloff, 2005). And also in the course of recovery from stroke, neuroplastic processes have shown to be paralleled by abnormal coherence within and between cortical sites (Nicolo et al., 2015; Wu et al., 2014).

4.2. Why do stroke patients show increased coupling between parietal and frontal areas during a grip task?

It is conceivable that connectivity patterns vary over time and depend both on the severity of stroke and the level of recovery thereafter. Previous studies on stroke recovery have found that in the acute stage, stroke patients have reduced facilitatory coupling from secondary motor areas to the contralateral (ipsilesional) M1; additionally, they experience reduced inhibitory coupling from secondary motor areas to the ipsilateral (contralesional) M1 (Rehme et al., 2011b). Recovery is accompanied by a normalization of this abnormal pattern but in the chronic stage, conditional on the degree of deficit, an enhanced inhibitory coupling from contralesional to ipsilesional M1 can be detected (Grefkes et al., 2008b; Rehme et al., 2011a). Albeit these abnormal connectivity patterns which help understand variable recovery patterns between stroke patients, we currently lack a precise neurophysiological framework. In the present study, we found that in a simple visuomotor grip task, stroke patients show an increased synchrony between the aIPS and M1 (Table 2), and with a higher residual motor deficit, this synchrony was also higher (Table 3, Fig. 3). Given the established importance of the parietal cortex for visuomotor and sensorimotor integration, both essential components in human everyday motor behaviour, this finding might add an important and conceptually plausible missing link.

It is likely that in the post-stroke brain, higher integrative demands are required for task performance that rely on specific features such as visuomotor translation of the cue position, somatosensory integration, hand shaping and visual feedback information processing into force adaptation, all of which have been related to parietal motor area activity also in the healthy human brain (Bernier et al., 2017; Klaes et al., 2015; Konen et al., 2013; Murata et al., 2000; Sakata and Kusunoki, 1992; Sakata et al., 1997; Taira et al., 1990; Vingerhoets, 2014). The visuomotor integrative role of the dorsal parietal cortex was further differentiated to provide corrective movement plans to goal perturbation (Tunik et al., 2008). Such on-line adaptive adjustments of force output to small changes in the bar height were likely stronger in the stroke patients (Supplemental Fig. 2).

Direct projections to distal hand motoneurons which provide the posterior parietal cortex with the potential to control motoneuron activity directly at the spinal level, have recently been detected in monkeys (Rathelot et al., 2017), undermining the parietal cortex as a 'command apparatus' for hand movements. The specific information is more effectively relayed if the windows for communication between the parietal cortex and primary motor areas are opening and closing at the same points in time, indicated by higher synchrony between the oscillations at aIPS and M1.

The plastic reorganization and remodeling process could likewise lead to a greater contribution of alternative motor tracts arising from frontal and parietal sites to the corticospinal tract (McNeal et al., 2010; Newton et al., 2006; Puig et al., 2017; Schulz et al., 2015; Schulz et al., 2012). We propose that by synchronizing independent neural computations across task-involved regions, which together give rise to corticospinal projections, the summation of spikes becomes more effective at driving postsynaptic neurons at lower spinal levels (Salinas and Sejnowski, 2001). Thereby, a lesion-induced loss of cortical signal generating areas and conducting fibers is compensated. Importantly, the above interpretations regarding synchronization as a mean for task-specific information relay across cortical sites and synchronization as a mean for maximizing effect of presynaptic spiking activity on lower motor neurons, are not mutually exclusive but could have overlapping and synergistic function.

4.3. What it the relevance of the frequency bands of coupled oscillations?

We a priori focussed our analysis on motor-relevant frequency bands based on existing studies pertaining to task-induced changes in the power or coherence spectrogram in stroke patients (Gerloff et al., 2006). The crucial characteristic of alpha is a functional inhibition or engagement of task-irrelevant areas by amplitude down- and upregulation, a view that is supported by ample experimental evidence across cognitive systems, species and brain locations. A higher alpha rhythm over the sensorimotor cortices is specifically reactive during motor tasks (termed the mu rhythm), whereas the lower, or classic alpha rhythm, is reactive in the visual and general attentive system. In the motor system, beta generally shows a high conformity and/or overlap with alpha rhythms, but a specific role has been carved out for corticospinal coherence especially during hold periods of motor tasks (Chen et al., 2013). Thus, a status quo view of beta signaling emerged, i.e. the signaling responsible for the maintenance of current sensorimotor or cognitive states (Engel and Fries, 2010). However, it was shown for both rhythms that local spiking activity is structured by the oscillation of peaks and troughs in a pulsed manner (Haegens et al., 2011; Miller et al., 2012), see above, compatible with the view that both play predominantly top-down directing roles, although clearly distinctive functions for each rhythm are not extractable from the literature. Rossiter et al. found reduced movement-related beta desynchronization (15–30 Hz) in contralateral (ipsilesional) M1 during a visually guided grip task in patients compared with control subjects which were also related to the degree of motor deficit (Rossiter et al., 2014). In our results, we found a similar qualitative relation, but the group difference was not statistically significant (mean TR-Pow 20 Hz M1 patients: −0.42, controls: −0.44; LME, $p = 0.67$). A few studies have investigated resting-state oscillatory phase coupling networks in stroke patients which revealed a predictive value of ipsi- and contralesional connectivity for motor recovery in the alpha band (8–12 Hz), (Westlake et al., 2012; Wu et al., 2011), low beta band (13–16 Hz) (Nicolo et al., 2015), high beta band (20–30 Hz (Wu et al., 2014), 24–33 Hz (Pellegrino et al., 2012)) or broadband beta (13–30 Hz) (De Vico Fallani et al., 2013).

Taken together, the similarity between the connection profiles across frequency bands is in accordance with current concepts of the rhythms' functional roles: disinhibition of local circuitry in motor-relevant areas, signal transmission for the maintenance of the constant force output throughout the hold phase of the grip task and constant integration of visual feedback and integration in the motor command.

4.4. Predictive value of parietofrontal connectivity for residual motor deficit

An additional finding of this study was that apart from aIPS-M1 functional coupling being higher in stroke patients compared with controls, the degree of coupling correlated with the residual motor deficit. This finding is consistent with aforementioned fMRI findings in frontal motor network architecture, where increased inhibitory coupling from contralesional to ipsilesional M1 was significantly and positively related to residual motor deficit (Rehme et al., 2011a). The increased aIPS-M1 coupling could be an expression of a task-specific network adaptation, meaning that the coupling is directly related to the visuomotor demands of the task. Alternatively, it could be an expression of post-stroke network reorganization that is incidentally revealed by this task. A causal involvement of aIPS-M1 coupling in meeting task demands is difficult to assess with pure observational techniques. However, since the experimental design included a task in which the applied grip force was 20% of the maximal grip force, we can conclude, that TR-Coh is not only related to the clinical impairment as measured by grip force and the NHP, but likewise related to the task specific requirement of force generation. However, this does not rule out the possibility that the M1-aIPS coupling is an unspecific property of the stroke-lesioned brain. Furthermore, the qualitative nature of high

parietofrontal connectivity remains to be elucidated: Is the high parietofrontal connectivity causing a functional impairment (maladaptive) or is it an (unsuccessful) attempt to generate motor output (adaptive). Such causal links can only be elucidated with brain stimulation (Di Pino et al., 2014) or neurofeedback (Enriquez-Geppert et al., 2017) protocols.

In our results, a low motor function was associated with high parietofrontal connectivity and a high motor function was associated to low parietofrontal connectivity. A high motor function in the chronic stage can either be attributed to a mild initial impact of the stroke or a good motor recovery. Therefore, we analyzed if the group of patients with a high motor function could be dissociated into well recovered (high motor recovery) and mildly affected (low motor recovery) patients based on their TR-Coh values. Such a pattern would be reflected in a different slope in the relationship between TR-Coh and residual motor function for patients with a high and low motor recovery. We did not find a significant relationship between motor recovery and residual motor function in explaining variance in TR-Coh three months after stroke. From this data it is attractive to speculate, that the downregulation of initially upregulated parietofrontal connectivity is a part of successful motor recovery. However, since we lack information on initial TR-Coh values, we are unable to confirm this point with the present study.

A longitudinal recording of EEG during the course of recovery could further explain if a) successful recovery goes along with a reduction of initially high parietofrontal connectivity or b) patients who do not recover from severe initial impairment upregulate parietofrontal connectivity over time.

Apart from those conceptual limitations regarding the interpretational scope of our study, another important limitation affects to spatial accuracy of our results: Source activity (and connectivity) between close targets are hard to unambiguously separate even with advanced spatial reconstruction methods of the EEG signal (Srinivasan et al., 2007). The present study benefits from previously identified individual peak motor coordinates in an overlapping patient and control participants population using the same motor task, thereby improving the spatial accuracy of the source reconstruction (Schulz et al., 2016). However, instead of making a strong argument for specific aIPS and M1 connectivity upregulation we want to emphasize "parietofrontal connectivity" on a system level. Also, the clinical heterogeneity of stroke patients necessitates much larger sample sizes for subgroup analyses, which we were unable to do even with the present cohort size ($n = 30$).

To summarize, the present findings provide evidence for enhanced parietofrontal coupling in the stroke-lesioned hemisphere during a visuomotor grip task which was correlated with residual motor deficit. This pattern of upregulation of parietofrontal coupling has now been reproduced in two completely independent measurement modalities (fMRI, EEG) and conceptual frameworks of connectivity in the brain (DCM, Coherence), thereby emphasizing the validity and importance of this connection for the post-stroke functional brain architecture. As visuomotor integration constitutes a major part of everyday gross motion and fine dexterous finger movement, this enhanced connectivity might subserve motor function in stroke survivors.

Conflicts of interest

Nothing to report.

Acknowledgements

Appendix A. Supplementary data

Supplementary data to this article can be found online at https://doi.org/10.1016/j.nicl.2018.03.006.

References

Arce-McShane, F.I., Ross, C.F., Takahashi, K., Sessle, B.J., Hatsopoulos, N.G., 2016. Primary motor and sensory cortical areas communicate via spatiotemporally coordinated networks at multiple frequencies. Proc. Natl. Acad. Sci. U. S. A. 113, 5083–5088.

Benjamini, Y., Hochberg, Y., 1995. Controlling the false discovery rate: a practical and powerful approach to multiple testing. J. R. Stat. Soc. 57, 289–300.

Bernier, P.M., Whittingstall, K., Grafton, S.T., 2017. Differential recruitment of parietal cortex during spatial and non-spatial reach planning. Front. Hum. Neurosci. 11, 249.

Bonnefond, M., Kastner, S., Jensen, O., 2017. Communication between brain areas based on nested oscillations. eNeuro 4.

Bonstrup, M., Schulz, R., Cheng, B., Feldheim, J., Zimerman, M., Thomalla, G., Hummel, F.C., Gerloff, C., 2015. Evolution of brain activation after stroke in a constant-effort versus constant-output motor task. Restor. Neurol. Neurosci. 33, 845–864.

Bonstrup, M., Schulz, R., Feldheim, J., Hummel, F.C., Gerloff, C., 2016. Dynamic causal modelling of EEG and fMRI to characterize network architectures in a simple motor task. NeuroImage 124, 498–508.

Chen, S., Entakli, J., Bonnard, M., Berton, E., De Graaf, J.B., 2013. Functional corticospinal projections from human supplementary motor area revealed by corticomuscular coherence during precise grip force control. PLoS One 8, e60291.

Corbetta, M., Shulman, G.L., 2002. Control of goal-directed and stimulus-driven attention in the brain. Nat. Rev. Neurosci. 3, 201–215.

Crone, N.E., Miglioretti, D.L., Gordon, B., Sieracki, J.M., Wilson, M.T., Uematsu, S., Lesser, R.P., 1998. Functional mapping of human sensorimotor cortex with electrocorticographic spectral analysis. I. Alpha and beta event-related desynchronization. Brain 121 (Pt 12), 2271–2299.

De Vico Fallani, F., Pichiorri, F., Morone, G., Molinari, M., Babiloni, F., Cincotti, F., Mattia, D., 2013. Multiscale topological properties of functional brain networks during motor imagery after stroke. NeuroImage 83, 438–449.

Di Pino, G., Pellegrino, G., Assenza, G., Capone, F., Ferreri, F., Formica, D., Ranieri, F., Tombini, M., Ziemann, U., Rothwell, J.C., Di Lazzaro, V., 2014. Modulation of brain plasticity in stroke: a novel model for neurorehabilitation. Nat. Rev. Neurol. 10, 597–608.

Engel, A.K., Fries, P., 2010. Beta-band oscillations—signalling the status quo? Curr. Opin. Neurobiol. 20, 156–165.

Enriquez-Geppert, S., Huster, R.J., Herrmann, C.S., 2017. EEG-neurofeedback as a tool to modulate cognition and behavior: a review tutorial. Front. Hum. Neurosci. 11, 51.

Fries, P., 2005. A mechanism for cognitive dynamics: neuronal communication through neuronal coherence. Trends Cogn. Sci. 9, 474–480.

Gerloff, C., Bushara, K., Sailer, A., Wassermann, E.M., Chen, R., Matsuoka, T., Waldvogel, D., Wittenberg, G.F., Ishii, K., Cohen, L.G., Hallett, M., 2006. Multimodal imaging of brain reorganization in motor areas of the contralesional hemisphere of well recovered patients after capsular stroke. Brain 129, 791–808.

Grefkes, C., Fink, G.R., 2011. Reorganization of cerebral networks after stroke: new insights from neuroimaging with connectivity approaches. Brain 134, 1264–1276.

Grefkes, C., Ritzl, A., Zilles, K., Fink, G.R., 2004. Human medial intraparietal cortex subserves visuomotor coordinate transformation. NeuroImage 23, 1494–1506.

Grefkes, C., Eickhoff, S.B., Nowak, D.A., Dafotakis, M., Fink, G.R., 2008a. Dynamic intra- and interhemispheric interactions during unilateral and bilateral hand movements assessed with fMRI and DCM. NeuroImage 41, 1382–1394.

Grefkes, C., Nowak, D.A., Eickhoff, S.B., Dafotakis, M., Kust, J., Karbe, H., Fink, G.R., 2008b. Cortical connectivity after subcortical stroke assessed with functional magnetic resonance imaging. Ann. Neurol. 63, 236–246.

Gross, J., Kujala, J., Hamalainen, M., Timmermann, L., Schnitzler, A., Salmelin, R., 2001. Dynamic imaging of coherent sources: studying neural interactions in the human brain. Proc. Natl. Acad. Sci. U. S. A. 98, 694–699.

Haegens, S., Nacher, V., Luna, R., Romo, R., Jensen, O., 2011. alpha-Oscillations in the monkey sensorimotor network influence discrimination performance by rhythmical inhibition of neuronal spiking. Proc. Natl. Acad. Sci. U. S. A. 108, 19377–19382.

Hummel, F., Gerloff, C., 2005. Larger interregional synchrony is associated with greater behavioral success in a complex sensory integration task in humans. Cereb. Cortex 15, 670–678.

Klaes, C., Kellis, S., Aflalo, T., Lee, B., Pejsa, K., Shanfield, K., Hayes-Jackson, S., Aisen, M., Heck, C., Liu, C., Andersen, R.A., 2015. Hand shape representations in the human posterior parietal cortex. J. Neurosci. 35, 15466–15476.

Konen, C.S., Mruczek, R.E., Montoya, J.L., Kastner, S., 2013. Functional organization of human posterior parietal cortex: grasping- and reaching-related activations relative to topographically organized cortex. J. Neurophysiol. 109, 2897–2908.

Kuznetsova, A., Brockhoff, P.B., Christensen, R.H.B., Package 'lmerTest', 2015. Tests in Linear Mixed Effects Models.

Makeig, S., Bell, A.J., Jung, T.-P., Sejnowski, T.J., 1996. Independent component analysis of electroencephalographic data. In: Touretzky, D., Mozer, M., Hasselmo, M. (Eds.), Advances in Neural Information Processing Systems. MIT Press, Cambridge, M.A., pp. 145–151.

McNeal, D.W., Darling, W.G., Ge, J., Stilwell-Morecraft, K.S., Solon, K.M., Hynes, S.M., Pizzimenti, M.A., Rotella, D.L., Vanadurongvan, T., Morecraft, R.J., 2010. Selective long-term reorganization of the corticospinal projection from the supplementary motor cortex following recovery from lateral motor cortex injury. J. Comp. Neurol.

518, 586–621.

Miller, K.J., Hermes, D., Honey, C.J., Hebb, A.O., Ramsey, N.F., Knight, R.T., Ojemann, J.G., Fetz, E.E., 2012. Human motor cortical activity is selectively phase-entrained on underlying rhythms. PLoS Comput. Biol. 8, e1002655.

Murata, A., Gallese, V., Luppino, G., Kaseda, M., Sakata, H., 2000. Selectivity for the shape, size, and orientation of objects for grasping in neurons of monkey parietal area AIP. J. Neurophysiol. 83, 2580–2601.

Newton, J.M., Ward, N.S., Parker, G.J., Deichmann, R., Alexander, D.C., Friston, K.J., Frackowiak, R.S., 2006. Non-invasive mapping of corticofugal fibres from multiple motor areas—relevance to stroke recovery. Brain 129, 1844–1858.

Nicolo, P., Rizk, S., Magnin, C., Pietro, M.D., Schnider, A., Guggisberg, A.G., 2015. Coherent neural oscillations predict future motor and language improvement after stroke. Brain 138, 3048–3060.

Pellegrino, G., Tomasevic, L., Tombini, M., Assenza, G., Bravi, M., Sterzi, S., Giacobbe, V., Zollo, L., Guglielmelli, E., Cavallo, G., Vernieri, F., Tecchio, F., 2012. Inter-hemispheric coupling changes associate with motor improvements after robotic stroke rehabilitation. Restor. Neurol. Neurosci. 30, 497–510.

Puig, J., Blasco, G., Schlaug, G., Stinear, C.M., Daunis, I.E.P., Biarnes, C., Figueras, J., Serena, J., Hernandez-Perez, M., Alberich-Bayarri, A., Castellanos, M., Liebeskind, D.S., Demchuk, A.M., Menon, B.K., Thomalla, G., Nael, K., Wintermark, M., Pedraza, S., 2017. Diffusion tensor imaging as a prognostic biomarker for motor recovery and rehabilitation after stroke. Neuroradiology 59, 343–351.

Rathelot, J.A., Dum, R.P., Strick, P.L., 2017. Posterior parietal cortex contains a command apparatus for hand movements. Proc. Natl. Acad. Sci. U. S. A. 114, 4255–4260.

Rehme, A.K., Eickhoff, S.B., Wang, L.E., Fink, G.R., Grefkes, C., 2011a. Dynamic causal modeling of cortical activity from the acute to the chronic stage after stroke. NeuroImage 55, 1147–1158.

Rehme, A.K., Fink, G.R., von Cramon, D.Y., Grefkes, C., 2011b. The role of the contralesional motor cortex for motor recovery in the early days after stroke assessed with longitudinal FMRI. Cereb. Cortex 21, 756–768.

Rehme, A.K., Eickhoff, S.B., Rottschy, C., Fink, G.R., Grefkes, C., 2012. Activation likelihood estimation meta-analysis of motor-related neural activity after stroke. NeuroImage 59, 2771–2782.

Rossini, P.M., Calautti, C., Pauri, F., Baron, J.C., 2003. Post-stroke plastic reorganisation in the adult brain. Lancet Neurol. 2, 493–502.

Rossiter, H.E., Boudrias, M.H., Ward, N.S., 2014. Do movement-related beta oscillations change after stroke? J. Neurophysiol. 112, 2053–2058.

R Team, 2015. RStudio: Integrated Development Environment for R. RStudio, Inc., Boston, MA.

Sakata, H., Kusunoki, M., 1992. Organization of space perception: neural representation of three-dimensional space in the posterior parietal cortex. Curr. Opin. Neurobiol. 2, 170–174.

Sakata, H., Taira, M., Kusunoki, M., Murata, A., Tanaka, Y., 1997. The TINS lecture. The parietal association cortex in depth perception and visual control of hand action. Trends Neurosci. 20, 350–357.

Salenius, S., Portin, K., Kajola, M., Salmelin, R., Hari, R., 1997. Cortical control of human motoneuron firing during isometric contraction. J. Neurophysiol. 77, 3401–3405.

Salinas, E., Sejnowski, T.J., 2001. Correlated neuronal activity and the flow of neural information. Nat. Rev. Neurosci. 2, 539–550.

Schulz, R., Park, C.H., Boudrias, M.H., Gerloff, C., Hummel, F.C., Ward, N.S., 2012. Assessing the integrity of corticospinal pathways from primary and secondary cortical motor areas after stroke. Stroke 43, 2248–2251.

Schulz, R., Koch, P., Zimerman, M., Wessel, M., Bonstrup, M., Thomalla, G., Cheng, B., Gerloff, C., Hummel, F.C., 2015. Parietofrontal motor pathways and their association with motor function after stroke. Brain 138, 1949–1960.

Schulz, R., Buchholz, A., Frey, B.M., Bonstrup, M., Cheng, B., Thomalla, G., Hummel, F.C., Gerloff, C., 2016. Enhanced effective connectivity between primary motor cortex and intraparietal sulcus in well-recovered stroke patients. Stroke 47, 482–489.

Siegel, M., Donner, T.H., Engel, A.K., 2012. Spectral fingerprints of large-scale neuronal interactions. Nat. Rev. Neurosci. 13, 121–134.

Srinivasan, R., Winter, W.R., Ding, J., Nunez, P.L., 2007. EEG and MEG coherence: measures of functional connectivity at distinct spatial scales of neocortical dynamics. J. Neurosci. Methods 166, 41–52.

Taira, M., Mine, S., Georgopoulos, A.P., Murata, A., Sakata, H., 1990. Parietal cortex neurons of the monkey related to the visual guidance of hand movement. Exp. Brain Res. 83, 29–36.

Tunik, E., Ortigue, S., Adamovich, S.V., Grafton, S.T., 2008. Differential recruitment of anterior intraparietal sulcus and superior parietal lobule during visually guided grasping revealed by electrical neuroimaging. J. Neurosci. 28, 13615–13620.

Vingerhoets, G., 2014. Contribution of the posterior parietal cortex in reaching, grasping, and using objects and tools. Front. Psychol. 5, 151.

Ward, N.S., 2017. Restoring brain function after stroke - bridging the gap between animals and humans. Nat. Rev. Neurol. 13, 244–255.

Ward, N.S., Brown, M.M., Thompson, A.J., Frackowiak, R.S., 2003. Neural correlates of outcome after stroke: a cross-sectional fMRI study. Brain 126, 1430–1448.

Westlake, K.P., Hinkley, L.B., Bucci, M., Guggisberg, A.G., Byl, N., Findlay, A.M., Henry, R.G., Nagarajan, S.S., 2012. Resting state alpha-band functional connectivity and recovery after stroke. Exp. Neurol. 237, 160–169.

Wu, W., Sun, J., Jin, Z., Guo, X., Qiu, Y., Zhu, Y., Tong, S., 2011. Impaired neuronal synchrony after focal ischemic stroke in elderly patients. Clin. Neurophysiol. 122, 21–26.

Wu, J., Srinivasan, R., Kaur, A., Cramer, S.C., 2014. Resting-state cortical connectivity predicts motor skill acquisition. NeuroImage 91, 84–90.